Synthesis, Characterization, and Direct Observation of Star Microgels

Paul A. Gurr, Greg G. Qiao,* and David H. Solomon

Polymer Science Group, Department of Chemical and Biomolecular Engineering, The University of Melbourne, Victoria, 3010, Australia

Shane E. Harton[†] and Richard J. Spontak*[,†,‡]

Departments of Materials Science & Engineering and Chemical Engineering, North Carolina State University, Raleigh, North Carolina 27695

Received February 19, 2003

ABSTRACT: The molecular sizes of four star microgels, synthesized by atom transfer radical polymerization of poly(methyl methacrylate) (PMMA) with ethylene glycol dimethacrylate as the cross-linker, have been investigated by light scattering methods and transmission electron microscopy (TEM). Gel permeation chromatography right-angle laser light scattering performed with a triple detector system and dynamic light scattering together confirm that individual particles of one star microgel in tetrahydrofuran and styrene solutions possess mean diameters of 31 and 18 nm, respectively. Complementary TEM reveals that another star microgel appears as discrete particles measuring 18−30 nm in diameter when added to styrene monomer subsequently polymerized to form a solid matrix. These particles likewise undergo macrophase separation to form microgel-rich domains consisting of nanoscale PMMA channels. Additional TEM examination of a star microgel deposited by dilute solution casting provides direct evidence for the existence of individual microgel molecules with a mean (dry) diameter of ∼15 nm.

Introduction

Current interest in star microgels can be attributed to their unique three-dimensional shape and highly branched structures.[1−3] Recent efforts have demonstrated that these interesting macromolecules can be effectively synthesized by controlled free radical polymerization using the "core-first" approach.[1,2,4−8] Controlled polymerizations refer to those methods developed in the past decade to produce polymers (especially those not amenable to living ionic polymerizations) with relatively narrow polydispersity ($\bar{M}_w/\bar{M}_n$).[9] Methods used to synthesize star microgels by controlled polymerization include nitroxide-mediated polymerization (NMP),[1,2] atom transfer radical polymerization (ATRP),[4−7] and reversible addition−fragmentation chain transfer polymerization (RAFT).[8] These methods are particularly attractive in the efficient preparation of star microgels since they permit synthesis under substantially less stringent conditions than those required for controlled ionic polymerizations and yet yield microgel molecules with narrow polydispersities (usually ∼1.5−2.0) and relatively uniform arm lengths.

The architecture of star microgels is responsible for the unique properties of such macromolecules, such as extremely low viscosity at very high molecular weight. In fact, a recent study[4b] has reported that star microgels exhibit particle-like behavior in solution; i.e., the viscosity of star microgel solutions closely resembles that of a suspension of discrete particles and is essentially size independent. The molecular weight of the linear arms comprising star microgels is usually on the order of 10 000−50 000. Since the number of arms attached to each microgel molecule ranges from 20 to 100, the resultant molecular weight of star microgels varies from a few hundred thousand to a few million. To better understand and exploit the applicability of these unique nonlinear macromolecules, their morphology must be elucidated. While the size determination of star microgels usually involves GPC measurements based on either right-angle laser light scattering (RALLS) or multiangle laser light scattering (MALLS),[4,6,7] it would be beneficial to complement such indirect morphological analyses by imaging individual molecules. Efforts, such as those spearheaded by Wooley and co-workers,[10] have probed the morphological characteristics of shell-cross-linked nanoparticles (with hollow cores), but no study to the best of our knowledge has provided direct visualization of star microgels with cross-linked cores. The present work employs RALLS, dynamic light scattering (DLS), and transmission electron microscopy (TEM) to explore the morphological characteristics of star microgel molecules.

Experimental Section

Materials. Methyl methacrylate (MMA) and ethylene glycol dimethacrylate (EGDMA) monomers were washed 3 times with 5% sodium hydroxide solution and once with water. The solutions were dried over $MgSO_4$, filtered, and distilled from calcium chloride. Purified monomers were stored in a freezer following distillation. *p*-Toluenesulfonyl chloride (*p*-TsCl) was dissolved in chloroform, diluted with petroleum ether (bp 40−60 °C), clarified with charcoal, filtered, concentrated, and collected by filtration. Styrene monomer was passed through an alumina column and subsequently distilled. 2,2′-Bipyridine (bpy) was purchased from Aldrich and used without further purification. All solvents were used after distillation.

Synthesis. Star microgels were prepared by the ATRP protocol with the "arms-first" approach, as described elsewhere.[7] Living poly(methyl methacrylate) (PMMA) arms were prepared by the polymerization of methyl methacrylate using *p*-TsCl as the initiator and CuCl/bpy as the catalyst. The living arms were then reacted with the cross-linker (EGDMA) to form

[†] Department of Materials Science & Engineering.
[‡] Department of Chemical Engineering.
* To whom correspondence should be addressed. E-mail gregghq@unimelb.edu.au and rich_spontak@ncsu.edu.

10.1021/ma030122m CCC: $25.00
Published on Web 06/25/2003

Table 1. Characteristics of PMMA Star Microgels by GPC with a Triple Detector System

star microgel	molar ratio of arms to EGDMA	$\bar{M}_n$ (arm)	$\bar{M}_n$ (microgel)	R_{gw} (nm)	$\bar{M}_w/\bar{M}_n$ (microgel)	f	conversion (arm → microgel)
A	1:10	16 900	485 000	15.5	1.08	25	84.9
B	1:15	57 200	5 630 000	39.8	1.07	85	57.9
C	1:15	107 000	3 320 000	90.7	1.02	28	43.3
D	1:15	62 300	1 070 000	24.1	1.17	15	55.7

the star microgel, which consisted of a central core surrounded by linear polymeric arms, also under ATRP conditions. The designations and molecular weights of the star microgels (A−D) synthesized in this fashion, as well as the ratio of microgel to attached linear PMMA present, are listed in Table 1. The detailed procedure for synthesizing microgel A is as follows:

Living PMMA Arms. A mixture of methyl methacrylate (10.0 mL, 0.093 mol), CuCl (0.020 g, 0.20 mmol), bpy (0.11 g, 0.70 mmol), and *p*-TsCl (0.090 g, 0.47 mmol) in *p*-xylene (5.0 mL) was added to a Schlenk flask and degassed by three freeze−pump−thaw cycles. The flask was then immersed in an oil bath at 100 °C and heated for 90 h. The reaction mixture was dissolved in THF (100 mL) and precipitated into MeOH (2 L). The precipitate was collected by vacuum filtration, and the precipitation was repeated to yield living PMMA polymer as a white solid (8.61 g, 92% yield). GPC (universal calibration): $\bar{M}_n$ = 16 900; $\bar{M}_w$ = 18 700; IV_w = 0.110; R_{gw} = 4.12 nm. ^{1}H NMR ($CDCl_3$, 400 MHz): δ 7.74 (d, J = 8.2 Hz, 0.018H, ArH), 7.36 (d, J = 8.0 Hz, 0.018H, ArH), 3.60 (s, 3H, OCH_3), 2.0−1.7 (m, 2H, CH_2), 1.02 (s, 0.45H, CH_3) 0.83 (s, 0.55H, CH_3).

Star Microgel A. A mixture of living PMMA polymer (1.97 g, 0.12 mmol), EGDMA (0.23 mL, 1.20 mmol), CuCl (7.8 mg, 0.079 mmol), and bpy (16.9 mg, 0.11 mmol) in *p*-xylene (10.0 mL) was added to a Schlenk flask containing a magnetic stirrer. The mixture was degassed by three freeze−pump−thaw cycles and then heated at 100 °C at atmospheric pressure. After 90 h a sample was removed from the reaction mixture and analyzed by gas chromatography to determine the conversion of the EGDMA cross-linker. The mixture was diluted with THF (20 mL), precipitated into MeOH (1 L), and collected by filtration to yield a colorless solid (1.86 g, 84% yield). GPC (TriSEC calibration): $\bar{M}_n$ = 485 000; $\bar{M}_w$ = 523 000; IV_w = 0.209; R_{gw} = 15.5 nm.

Characterization. *Gel Permeation Chromatography−Right-Angle Laser Light Scattering (GPC-RALLS).* The GPC measurements were conducted in THF using a Waters 717 Plus Autosampler, a Waters 510 HPLC pump equipped with three Phenomenex phenogel columns (50, 10^3, and 10^5 nm) in series with a Wyatt Dawn F laser photometer operated at 90°, and in parallel with a Waters 410 differential refractometer (RI) and a Viscotek T50A differential viscometer, which together provided a triple detector system. Data acquisition and analysis were performed with the Viscotek TriSEC software, and all three detectors were calibrated with PMMA standards of narrow molecular weight distribution and known intrinsic viscosity.

Dynamic Light Scattering (DLS). Dynamic light scattering measurements were performed using a Malvern 4700 unit with a 10 mW Ar^+ ion laser operated at 488 nm. Analysis was performed at an angle of 90° and a constant temperature of 25 °C. Dilute particle concentrations ensure that multiple scattering and particle−particle interactions can be considered negligible during data analysis. The particle concentration was adjusted so that the scattering from the particles exceeded that from residual linear polymer by several orders of magnitude.

Transmission Electron Microscopy (TEM). Specimens for analysis by TEM were prepared by two different approaches. In the first, microgels A to D were embedded in polystyrene (PS). Dry microgel powder was added to styrene monomer at a concentration of 2 mg/mL. After thorough mixing at ambient temperature, the styrene was polymerized at 60 °C with 2,2′-azobis(isobutyronitrile) (AIBN) as the initiator at a concentration of 6 mg AIBN/mL of styrene. The resultant PS blocks were sectioned at ambient temperature in a Reichert-Jung Ultracut-S ultramicrotome, and the sections were floated onto Cu TEM grids and subsequently exposed to the vapor of 0.5% RuO_4(aq), which selectively stains the phenyl rings of PS, for 7 min. The second preparation strategy eliminated the need for an embedding medium by casting star microgel A directly from a 0.5% w/v toluene solution. A drop of solution was added to a carbon-coated Cu grid and the toluene rapidly evaporated, thereby depositing a dispersion of microgel particles on the carbon substrate. Images of specimens produced according to both protocols were acquired on a Zeiss EM902 electron spectroscopic microscope operated at 80 kV and energy-loss (ΔE) settings of 0−40 eV. Negatives were digitized at 600 dpi, and the corresponding images were analyzed and prepared for presentation by several software packages, including Image (National Institutes of Health), Digitalmicrograph (Gatan), and Photoshop (Adobe).

Results and Discussion

Star microgels A−D have been synthesized using the ATRP method in two steps. In the first step, linear living polymer, required as the arm precursor for the star microgels, was prepared by polymerizing methyl methacrylate monomer with *p*-TsCl/CuCl/bpy in a *p*-xylene solution at 100 °C. This polymerization usually reaches more than 90% conversion after 72 h to yield living arms with narrow polydispersity ($\bar{M}_w/\bar{M}_n$ < 1.1). The purified living arms were subsequently cross-linked with EGDMA to form star microgels also under similar ATRP conditions at 100 °C. After 90 h, the conversion from linear chains to microgels is usually ∼90%. Details of the synthesis are provided in the Experimental Section, and the ratio of microgel to attached linear PMMA in microgels A−D is listed in Table 1. Star microgel A, synthesized with linear arms with $\bar{M}_n$ = 16 900, is used for illustrative purposes throughout this study. The conversion from linear chains to microgel molecules is about 85% in this case. Star microgels B−D have been synthesized with arms of substantially higher $\bar{M}_w$, ranging from ca. 50 000 to 100 000. These high-molecular-weight chains reduce the arm → microgel conversion to ∼50%.

The absolute molecular weight, the number of arms, and the gyration radius of star microgels A−D have been measured by GPC-RALLS in tetrahydrofuran (THF), and the results are included in Table 1. A representative GPC trace collected from star microgel A is displayed in Figure 1. Star microgel A with $\bar{M}_n \approx$ 0.5 million appears at a low retention time of 19.2 min, and its gyration radius (R_{gw}) is calculated to be 15.5 nm (31 nm diameter). About 15% unconverted linear PMMA arms ($\bar{M}_n$ = 16 900) appear at a retention time of 22.6 min and permit quantitation of the arm → microgel conversion. The polydispersity of star microgel A is relatively low (∼1.08), as anticipated from the ATRP procedure employed. Star microgels B−D possess molecular weights ranging from 1.0 to 5.6 million and corresponding gyration radii ranging from 24 to 91 nm. The average number of arms on each microgel (f) is deduced from the ratio of the molecular weight of the star microgel relative to that of the linear arms measured by the GPC triple detector system and varies from 15 to 85.

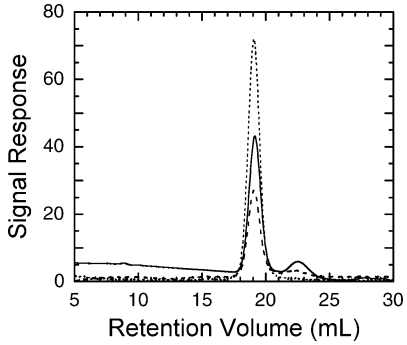

Figure 1. GPC traces of star microgel A obtained from a triple detector system: refractive index (RI, solid line), differential pressure (DP, dashed line), and light scattering (LS, dotted line).

We have recently reported that the size of star microgels is not necessarily proportional to molecular weight.[4b] While the configuration of star microgels has never been directly observed, these macromolecules are prepared in such fashion so that each arm attaches to the core at only one end, in which case the structure of the microgel molecule is envisaged to consist of a central core surrounded by attached linear polymer arms. Since star−star coupling[5] could also occur during microgel formation, direct observation of star microgels at the molecular level is required to understand the mechanism by which microgels form and how to interpret results acquired from indirect (e.g., DLS) analytical methods. To achieve this, star microgels A−D have been embedded in PS as described above. Contrast-inverted TEM images of these specimens are presented in Figure 2a−d, respectively, with Figure 2d showing more detail over a larger specimen area. Contrast inversion is used here to facilitate identification of the unstained (dark) PMMA in RuO_4-stained (light) PS.

Several features of these images warrant discussion. The first is that the star microgels, along with the residual linear PMMA, clearly undergo macrophase separation from the PS matrix to form micrometer-scale dispersions. This observation is consistent with the Flory−Huggins χ parameter for PMMA/PS,[11] which is estimated to be about 0.0182 at the T_g of PS (taken as 100 °C). These dispersions are not very pure and appear to consist of PMMA channels measuring about 16−20 nm across. The channels within the dispersions serve to separate adjacent PS-rich regions and are strikingly reminiscent of those previously observed[12] in macrophase-separated blends of PS and a disordered block copolymer. Similarly arranged macroscale dispersions are present in each of the microgel specimens prepared in this fashion, as evidenced by the images displayed in Figure 2a−d. Note, however, that the size of the dispersions, as well as that of the PS occlusions located within the dispersions, is sensitive to the details (molecular weight, conversion, and number of arms) of the star microgel embedded (see Table 1).

Other features of interest in Figure 2d are fine nanoscale strands, or filaments, of PMMA residing in close proximity to the dispersion. These strands, presumed to constitute the precursor to the macroscale dispersions, confirm that phase segregation between the PS matrix and the PMMA chains/star microgels most likely occurs as a consequence of growing PS chains during the in-situ embedding. An increase in the molecular weight of the PS promotes not only greater thermodynamic incompatibility but also an increase in matrix viscosity, which explains why some PMMA was frozen-in as ill-formed strands, rather than discrete dispersions. One last noteworthy characteristic of Figure 2d is the existence of discrete, dark dispersions measuring 18−30 nm in diameter. Several of these features are highlighted in the image to facilitate identification. It is comforting that these nanoscale dispersions, interpreted as individual star microgel molecules, are of the same size scale as the star microgel molecules discerned independently by complementary GPC-RALLS analysis. The apparent difference in size (18−30 nm from TEM and 48 nm from GPC-RALLS) may reflect the difference in chemical environment, since the microgel molecules are expected to contract (relative to their unperturbed size) in PS due to the thermodynamically poor environment.

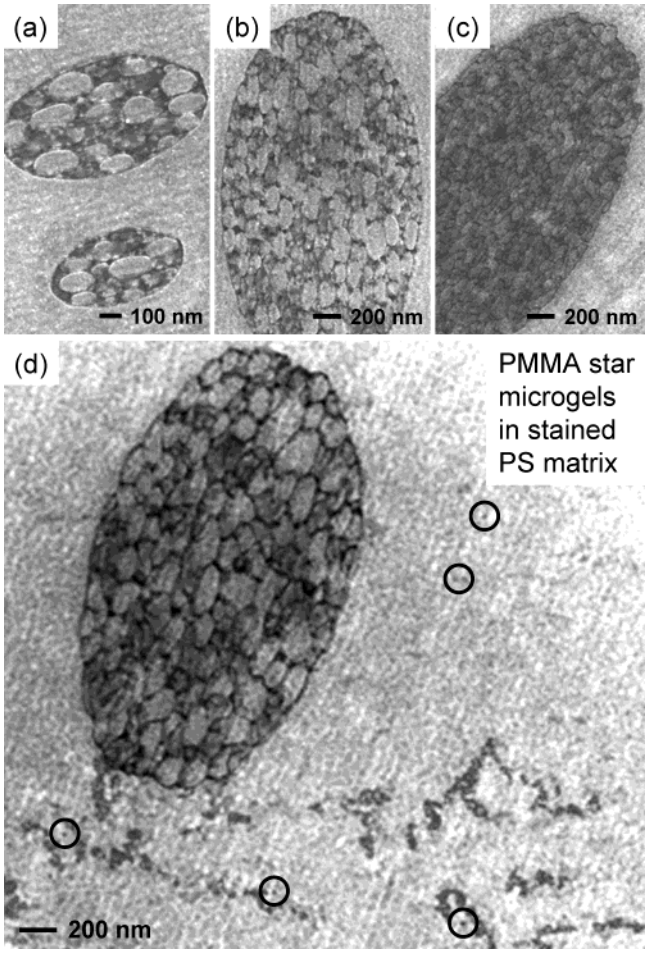

Figure 2. A series of contrast-reversed TEM images of PMMA star microgels (dark) embedded in RuO_4-stained PS (light): (a) star microgel A, (b) star microgel B, (c) star microgel C, and (d) star microgel D. The background lines evident in each image represent a specimen preparation artifact. In (d), several discrete microgel particles within the PS matrix are circled to facilitate identification.

To confirm that these macrophase-separated microgel-rich domains are formed during styrene polymerization, the characteristics of star microgel A have been investigated by DLS in a styrene monomer solution. Figure 3 shows size distributions based on scattered intensity, volume, and number, and the respective mean diameters extracted from these measurements are 17.9, 12.7, and 10.3 nm. Thus, the diameter of the star microgel A discerned from the scattered intensity is on the same size scale as that deduced from the GPC-RALLS

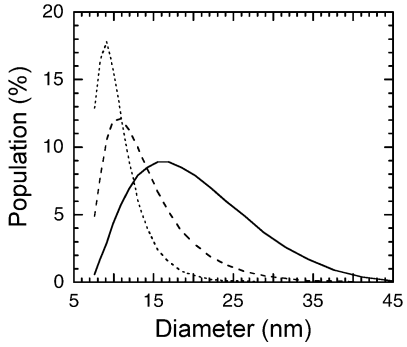

Figure 3. Size distributions of star microgel A according to DLS analysis derived on the basis of intensity (solid line), volume (dashed line), and number (dotted line). Mean diameters extracted from this analysis are provided in the text.

measurement for the same microgel in THF (31 nm) and from the TEM analysis for star microgel D in PS (18−31 nm). The DLS results also demonstrate that no micrometer-size particles are present, indicating that the PMMA chain/microgel solution in styrene monomer is homogeneous without any evidence of phase separation. Although ca. 15% of the PMMA exists as unconverted linear chains due to their low molecular weight, their contribution to the DLS signature of the solution is very small relative to that of the microgels, and their effect on the results is therefore negligible.

Since the embedded microgels undergo macrophase separation in the presence of PS, we now turn our attention to the TEM specimens prepared by direct casting of a dilute toluene solution. In this work, we avoid the use of negative stains to enhance image contrast due to the very high potential for artifact development. A representative zero-loss[13,14] ($\Delta E = 0$ eV) TEM image of star microgel A is provided in Figure 4a and reveals that many of the particles deposited in this fashion range from ca. 10 to 20 nm in size. A 3× enlargement of several particles is included as an inset to permit closer examination of the particles, which appear relatively diffuse. Such diffuseness is attributable to the compressible nature of the particles, since the particles are highly swollen in toluene and then collapse upon casting and subsequent drying. It is important to realize that (i) this image is not contrast-reversed as in Figure 2 and (ii) the electron contrast evident in this image is due solely to specimen thickness variation, since no staining agent is employed. Statistical analysis of the particle size distribution determined by measuring ∼400 microgel particles observed in images collected from multiple grid squares in two different TEM grids yields the histogram shown in Figure 4b. The distribution is surprisingly narrow, yielding a mean diameter ($\bar{d}$) of 15.4 nm and a standard deviation (σ) of 5.4 nm.

The particle dimensions reported in Figure 4b implicitly presume a spherical morphology, which is highly unlikely considering particle deformability. Indeed, close examination of Figure 4a confirms that the particles vary (slightly) in optical density, thereby confirming variation in particle height. In related studies, Wooley and co-workers[10] have conclusively demonstrated that shell-cross-linked particles, with hollow cores, can flatten markedly (exhibiting a diameter:height aspect ratio in excess of 10:1), upon deposition onto a hard (mica) surface. We likewise expect that our star microgels will undergo some degree of deformation upon deposition from solution but intuitively expect it to be less extensive than that of shell-cross-linked "nanocages" since the particle core is both occupied and cross-linked. A Beer−Lambert analysis of relative optical densities in unaltered TEM images (the one displayed in Figure 4a is contrast-enhanced) reveals that, if the thickness (t) of the substrate film is taken as 20 nm, the particle height in the z-direction (z is parallel to the electron beam) is estimated to range from about 4 to 21 nm, with an average height of ∼12 nm. [An increase in t serves to increase the value of these calculated heights.] This relatively simplistic analysis yields results that are consistent with our expectation that the deformation of star microgel particles upon deposition is, on average, less pronounced relative to hollow-core, shell-cross-linked particles. A more detailed analysis of star microgel morphology is forthcoming.

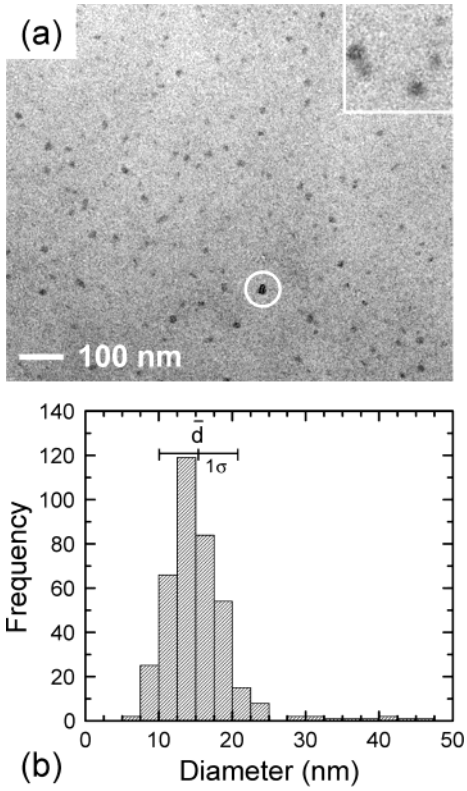

Figure 4. (a) A zero-loss TEM image of nanoscale star microgel A deposited from toluene on a carbon-coated grid and (b) the corresponding particle size distribution discerned from several images such as the one presented in (a). Included in (a) are a 3× enlargement of the particles and an example of an artifact (circled) excluded from the particle size analysis. The mean particle diameter ($\bar{d}$) and one standard deviation (σ) are identified in (b).

Another issue to consider here is that the mean diameter of the star microgel particles as determined by TEM is smaller than, but nonetheless in fair quantitative agreement with, the results obtained from the accompanying GPC-RALLS and DLS analyses in Figures 1 and 3, respectively. This size disparity may reflect the difference in conformation of the star microgel in the (dried) solid state and in solution. In solution, all arms of the microgel can be solvated and therefore occupy a relatively large excluded volume. In the solid state, however, the arms are most likely collapsed on the outer surface of the core, in which case the particles appear smaller. Such size disparity is expected to be more pronounced for a linear polymer, since the coil would occupy a larger swollen volume in solution. With

slight differences in observed particle sizes notwithstanding, this is the first direct observation of individual star microgel molecules generated by a controlled polymerization method. Further studies designed to differentiate the arms from the core using similar imaging methods, as well as with atomic force microscopy,[10] with model materials synthesized for such investigation are presently underway and will be reported in due course.

Conclusions

A series of star microgels prepared from PMMA as arms and EGDMA as the cross-linker have been synthesized and investigated to determine individual particle sizes in solution and in the solid state. Gel permeation chromatography performed using a triple detector system reveals that the number-average molecular weights of these microgels range from about 0.5 to 5.6 million, whereas GPC-RALLS measurements conducted in THF show that the corresponding microgel molecules measure from ∼30 to 180 nm in diameter. Results obtained from DLS of one of the star microgels in styrene solution yield a mean diameter of about 18 nm. Polymerizing the matrix of star microgels in styrene solution promotes macrophase separation and the formation of microgel-rich domains. According to TEM, the estimated size of individual star microgel D particles in the PS matrix is about 18−30 nm. Direct solution casting and subsequent TEM observation yields images of individual microgel molecules possessing a mean (dry) diameter of ∼15 nm in the solid state.

Acknowledgment. We thank Dr. David Dunstan for performing the DLS. Financial support to the University of Melbourne team from the SPIRT program of the Australian Research Council with the support of DuPont is greatly acknowledged.

References and Notes

(1) (a) Abrol, S.; Kambouris, P.; Looney, M.; Solomon, D. *Macromol. Rapid Commun.* **1997**, *18*, 755. (b) Solomon, D. H.; Abrol, S.; Kambouris, P. A.; Looney, M. G. WO 98/31739, 1998, The University of Melbourne, *A Process for Preparing Polymeric Microgels*. (c) Abrol, S.; Caulfield, M.; Qiao, G.; Solomon, D. *Polymer* **2001**, *42*, 5987.

(2) (a) Pasquale, A. J.; Long, T. E. *J. Polym. Sci., Part A: Polym. Chem.* **2001**, *39*, 216. (b) Tsoukatos, T.; Pispas, S.; Hadjichristidis, N. *J. Polym. Sci., Part A: Polym. Chem.* **2001**, *39*, 320. (c) Bosman, A. W.; Heumann, A.; Klaerner, G.; Fréchet, J. M. J.; Hawker, C. J. *J. Am. Chem. Soc.* **2001**, *123*, 6461. (d) Bosman, A. W.; Vestberg, R.; Heumann, A.; Fréchet, J. M. J.; Hawker, C. J. *J. Am. Chem. Soc.* **2003**, *125*, 715.

(3) Hawker, C. J.; Bosman, A. W.; Harth, E. *Chem. Rev.* **2001**, *101* 3661.

(4) (a) Solomon, D. H.; Qiao, G. G.; Abrol, S. WO 99/58588, 1999, The University of Melbourne, *Process for Microgel Preparation*. (b) Gurr, P. A.; Mills, M. F.; Qiao, G. G.; Solomon, D. H. *Polym. Prepr.* **2003**, *44*, 800; *Macromolecules*, submitted for publication.

(5) (a) Xia, J.; Zhang, X.; Matyjaszewski, K. *Macromolecules* **1999**, *32*, 4482. (b) Zhang, X.; Xia, J.; Matyjaszewski, K. *Macromolecules* **2000**, *33*, 2340.

(6) Baek, K.-Y.; Kamigaito, M.; Sawamoto, M. *Macromolecules* **2001**, *34*, 215; **2001**, *34*, 7629; **2002**, *35*, 1493.

(7) Baek, K.-Y.; Kamigaito, M.; Sawamoto, M. *J. Polym. Sci., Part A: Polym. Chem.* **2002**, *40*, 633; **2002**, *40*, 1972; **2002**, *40*, 2245.

(8) Barner-Kowollik, C.; Vana, P.; Davis, T. P. 224th ACS Nat. Mtg., Boston, MA, Aug 2002.

(9) Hanns, F. *Chem. Rev.* **2001**, *101* 3581 and references therein.

(10) (a) Huang, H.; Remsen, E. E.; Kowalewski, T.; Wooley, K. L. *J. Am. Chem. Soc.* **1999**, *121*, 3805. (b) Zhang, Q.; Remsen, E. E.; Wooley, K. L. *J. Am. Chem. Soc.* **2000**, *122*, 3642.

(11) Balsara, N. P. In *Physical Properties of Polymers Handbook*; Mark, J. E., Ed.; AIP Press: New York, 1996.

(12) Laurer, J. H.; Ashraf, A.; Smith, S. D.; Spontak, R. J. *Langmuir* **1997**, *13*, 2250.

(13) Reimer, L. *Energy-Filtering Transmission Electron Microscopy*; Springer-Verlag: Berlin, 1995.

(14) (a) Du Chesne, A. *Macromol. Chem. Phys.* **1999**, *200*, 1813. (b) Thomann, R.; Spontak, R. J. In *Science, Technology and Education of Microscopy: An Overview*; Mendez-Vilas, A., Ed.; Formatex: Badajoz, Spain, in press.

MA030122M